Transition-State Electronic Structures in S_N2 Reactions

Zheng Shi and Russell J. Boyd*

Contribution from the Department of Chemistry, Dalhousie University, Halifax, Nova Scotia, Canada B3H 4J3. *Received August 15, 1988*

Abstract: The topological definition of an atom in a molecule is used to calculate the charge on entering and leaving groups at the TS of S_N2 reactions. The systems studied are $N^- + CH_3X \rightarrow CH_3N + X^-$, where N, X = H, F, Cl, and OH. The calculations were done at the RHF and MP2 levels with extended basis sets that include diffuse and polarization functions. It is shown that the charges on entering and leaving groups are related to the position of the TS along the reaction coordinate and that the charges are not equal. The integrated charges are also used to estimate upper bounds to the contributions of the reactant and product configurations to the Shaik and Pross TS wave function. Charges obtained from the Mulliken population analysis are usually smaller than the integrated charges obtained from the theory of atoms in molecules. Qualitative differences between the two sets of data are noted, and the source of the differences explained. Also the electron density at the C-X bond critical point in the TS is shown to be related to the bond length and to the position of the TS along the reaction coordinate.

Transition-state theory has achieved widespread acceptance as a tool for the interpretation of chemical reaction rates and has led to much insight into chemical and physical processes.[1,2] The fundamental assumptions[3] involved in transition state (TS) theory are that molecules must traverse saddle points (transition states) of the potential energy surface and that the rate of reaction is proportional to the concentration of molecules in the TS, which, in turn, is in "quasi-equilibrium" with the reactants. Hence, the TS is the focus of the entire theory. Difficulties associated with direct measurements of TS's have impelled efforts to discover the relationship between reactants, products, and TS's and to predict the position and properties of TS's. The most famous postulate relating to transition states, due to Leffler and Hammond,[4,5] states that the properties of the TS are intermediate between reactant and product and are related to the position of the TS along the reaction coordinate.

Recently, Shaik and Pross[6-8] proposed a valence bond configuration mixing model, in which a reaction profile is formed from a linear combination of valence bond configurations and the TS occurs in the vicinity of the intersection point of the reactant-like and product-like energy curves. For simple S_N2 reactions

$$N^- + R\text{-}X \rightarrow N\text{-}R + X^-$$

where N^- is the entering nucleophile and X^- is the leaving group, the important configurations are

$$\underset{\mathbf{1}}{N:^- R\cdot\cdot X}, \qquad \underset{\mathbf{2}}{N\cdot\cdot R\ X:^-}, \qquad \underset{\mathbf{3}}{N:^- R^+ X:^-}, \qquad \underset{\mathbf{4}}{N\cdot\ R:^-\cdot X}$$

and the TS wave function is approximated by

$$\Psi_{TS} \approx a'\{2^{-1/2}(\psi_1 + \psi_2)\} + b'\psi_3 + c'\psi_4, \qquad (1)$$

where

$$(a')^2 + (b')^2 + (c')^2 = 1 \text{ and } a' > b', c'$$

The form of the Shaik and Pross[9] TS wave function assumes that the charges on N and X in the TS are equal and not related to the position of the TS along the reaction coordinate. This statement is, however, in conflict with the Hammond-Leffler postulate.

In this paper, we present the results of ab initio calculations and atomic charges calculated by application of the theory of atoms in molecules[10-12] and standard Mulliken population analysis for 16 model S_N2 reactions. The purpose is to provide further insight into the electronic structures of the TS's of S_N2 reactions and to compare integrated charges based on the theory of atoms in molecules with Mulliken gross atomic charges.

Methods and Calculations

Bader et al. have proposed a molecular structure theory,[10-12] in which atoms and bonds are uniquely defined in terms of the topology of the molecular electron density distribution. According to the theory, an atom is defined as a real space surrounded by a zero-flux surface of the electron density gradient. Integration of the electron density within an atomic surface yields the total number of electrons on the atom. Moreover, other atomic properties can also be calculated by integrating the corresponding densities within the atomic surface.

Furthermore bonded atoms are linked by bond paths which are the gradient paths of the electron density originating at critical points, points where the gradient of the electron density vanishes, and terminating at nuclei. These critical points are called bond critical points. Moreover the value of the electron density at a bond critical point is related to the bond order and bond strength.[13-15]

In this work, we have used the theory of atoms in molecules to study the electronic structures of the transition states of the following reactions

$$N^- + CH_3X \rightarrow CH_3N + X^-$$

where N, X = H, F, Cl, OH. Thus, our study includes four symmetric complexes in which N and X are identical and 12 asymmetric complexes in which N and X are different (Figure 1).

Calculations were carried out at the RHF (restricted Hartree-Fock) and MP2 (second-order Møller-Plesset) levels using the GAUSSIAN 80[16] and GAUSSIAN 86[17] computer programs. Standard 6-31G basis sets were used with s and p (s only for hydrogen) diffuse functions[18] and d (p only

(1) Laidler, K. J.; King, M. C. *J. Phys. Chem.* **1983**, *87*, 2657.
(2) Truhlar, D. G.; Hase, W. L.; Hynes, J. T. *J. Phys. Chem.* **1983**, *87*, 2664.
(3) Leffler, J. E.; Grunwald, E. *Rates and Equilibria of Organic Reactions*; John Wiley & Sons Inc.: 1963.
(4) Leffler, J. E. *Science* **1953**, *117*, 340.
(5) Hammond, G. S. *J. Am. Chem. Soc.* **1955**, *77*, 334.
(6) Shaik, S. S.; Pross, A. *J. Am. Chem. Soc.* **1982**, *104*, 2708.
(7) Pross, A.; Shaik, S. S. *Acc. Chem. Res.* **1983**, *16*, 363.
(8) Shaik, S. S. *Prog. Phys. Org. Chem.* **1985**, *15*, 197.
(9) Pross, A.; Shaik, S. S. *Tetrahedron Lett.* **1982**, *23*, 5467.
(10) Bader, R. F. W.; Nguyen-Dang, T. T.; Tal, Y. *J. Chem. Phys.* **1979**, *70*, 4316.
(11) Bader, R. F. W.; Nguyen-Dang, T. T.; Tal, Y. *Rep. Prog. Phys.* **1981**, *44*, 893.
(12) Bader, R. F. W. *Acc. Chem. Res.* **1985**, *18*, 9.
(13) Bader, R. F. W.; Slee, T. S.; Cremer, D.; Kraka, E. *J. Am. Chem. Soc.* **1983**, *105*, 5061.
(14) Boyd, R. J. *Studies Org. Chem.* **1987**, *31*, 485.
(15) Knop, O.; Boyd, R. J.; Choi, S. C. *J. Am. Chem. Soc.* **1988**, *110*, 7299.
(16) Binkley, J. S.; Whiteside, R. A.; Krishnan, R.; Seeger, R.; DeFrees, D. J.; Schlegel, H. B.; Topiol, S.; Kahn, L. R.; Pople, J. A. GAUSSIAN 80; Carnegie-Mellon Quantum Chemistry Publishing Unit: Pittsburgh, PA.
(17) Frisch, M. J.; Binkley, J. S.; Schlegel, H. B.; Raghavachari, K.; Melius, C. F.; Martin, R. L.; Stewart, J. J. P.; Bobrowicz, F. W.; Rohlfing, C. M.; Kahn, L. R.; DeFrees, D. J.; Seeger, R.; Whiteside, R. A.; Fox, D. J.; Fleuder, E. M.; Pople, J. A. GAUSSIAN 86; Carnegie-Mellon Quantum Chemistry Publishing Unit: Pittsburgh, PA, 1984.
(18) Clark, T.; Chandrasekhar, J.; Spitznagel, G. W.; Schleyer, P. v. R. *J. Comput. Chem.* **1983**, *4*, 294.

0002-7863/89/1511-1575$01.50/0

Table I. Properties at the Transition States of S_N2 Reactions

			R_{C-X}[b]		$-Q_X$[c]				ρ_{C-X}[d]			r_{C-X}[e]		
$(N\cdots R\cdots X)^-$	ΔE[a]	ΔH[a]	RHF	MP2	RHF	MP2′	MP2	MPA	RHF	MP2′	MP2	RHF	MP2′	MP2
$(H\cdots R\cdots H)^-$	0.0000	0.0000	1.690	1.589	0.60	0.52	0.52	0.72	0.068	0.071	0.086	1.351	1.286	1.189
$(HO\cdots R\cdots H)^-$	0.0427	0.0450	1.791	1.803	0.67	0.59	0.64	0.63	0.054	0.058	0.054	1.512	1.456	1.446
$(F\cdots R\cdots H)^-$	0.0742	0.0830	1.874	1.928	0.71	0.63	0.70	0.68	0.045	0.048	0.042	1.608	1.533	1.592
$(Cl\cdots R\cdots H)^-$	0.1424	0.1541	2.235	2.152	0.80	0.72	0.72	0.71	0.023	0.024	0.027	1.941	1.883	1.793
$(H\cdots R\cdots F)^-$	−0.0742	−0.0830	1.764	1.696	0.83	0.72	0.68	0.70	0.090	0.105	0.123	1.945	1.853	1.818
$(HO\cdots R\cdots F)^-$	−0.0284	−0.0380	1.795		0.85	0.74		0.74	0.081	0.095		1.986	1.903	
$(F\cdots R\cdots F)^-$	0.0000	0.0000	1.846	1.836	0.86	0.76	0.76	0.77	0.071	0.084	0.086	2.019	1.943	1.937
$(Cl\cdots R\cdots F)^-$	0.0608	0.0711	2.126		0.93	0.85		0.87	0.040	0.046		2.191	2.143	
$(H\cdots R\cdots Cl)$	−0.1424	−0.1541	2.086	2.027	0.64	0.54	0.51	0.54	0.086	0.092	0.105	2.343	2.243	2.183
$(HO\cdots R\cdots Cl)^-$	−0.0918	−0.1092	2.103		0.66	0.56		0.51	0.081	0.087		2.393	2.294	
$(F\cdots R\cdots Cl)^-$	−0.0608	−0.0711	2.133		0.68	0.58		0.54	0.075	0.081		2.428	2.329	
$(Cl\cdots R\cdots Cl)^-$	0.0000	0.0000	2.394		0.79	0.70		0.73	0.043	0.047		2.657	2.571	
$(H\cdots R\cdots OH)^-$	−0.0427	−0.0450	1.890	1.821	0.78	0.68	0.64	0.65	0.081	0.089	0.106	2.044	1.955	1.905
$(HO\cdots R\cdots OH)^-$	0.0000	0.0000	1.931		0.80	0.71		0.70	0.071	0.079		2.099	2.016	
$(F\cdots R\cdots OH)^-$	0.0284	0.0380	1.990		0.83	0.74		0.75	0.061	0.068		2.146	2.069	
$(Cl\cdots R\cdots OH)^-$	0.0918	0.1092	2.267		0.90	0.82		0.85	0.034	0.038		2.327	2.273	

[a] Energies in hartrees ($1E_h$ = 2625.5 kJ mol^{-1}). [b] Optimized C–X bond lengths in Å. [c] The first three entries correspond to the atomic charge on X obtained by integration, while the fourth entry refers to the charge obtained by Mulliken population analysis. [d] $\rho(r)$ at C–X bond critical point in atomic units. [e] Distance between X and C–X bond critical point in atomic units (1 au = 0.529177 Å).

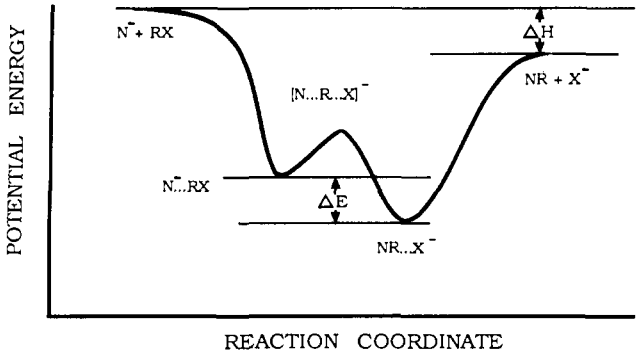

Figure 1. Schematic potential energy surface of a gas-phase S_N2 reaction.

for hydrogen) polarization functions[19] added to carbon and to entering and leaving groups. Thus, the 6-31++G** basis set[18] was chosen for the central carbon atom and the entering and leaving groups, while the 6-31G basis set was used for the three methyl hydrogen atoms. Diffuse functions were included in the basis set because they are known to be important for describing the electronic structures of anions containing first-row elements.[18,20,21] Geometries were fully optimized subject to C_{3v}, C_s, and C_2 symmetry constraints. The optimized geometries are shown in Figure 2. Topological properties were calculated by using the PROAIM[22] package and the modified PROAIM[23] package with all single and double excitations included. All calculations were performed on Perkin-Elmer 3230 and VAX 8800 computers.

Results and Discussion

Several theoretical levels have been used in this research. Results denoted by RHF were obtained with Hartree–Fock wave functions, and results denoted by MP2′ were obtained from second-order Møller–Plesset wave functions generated at the RHF optimized geometries (that is, MP2/6-31++G**//HF/6-31++G** in standard notation), whereas the MP2 results were obtained at the optimized second-order Møller–Plesset geometries (i.e., MP2/6-31++G**//MP2/6-31++G** in standard notation).

The computed properties at the transition states of selected S_N2 reactions are listed in Table I. The RHF energy difference between the two ion–molecule complexes, $\Delta E = E(NR\cdots X^-) - E(N^-\cdots RX)$, is followed by the RHF energy change for the gas-phase reaction, $\Delta H = [E(NR) + E(X^-)] - [E(N^-) + E(RX)]$. The C–X internuclear distance at the $(N\cdots R\cdots X)^-$ transition state, calculated at both the RHF and MP2 levels, is followed by the charge on the leaving group (Q_X) and the electron density at the C–X bond critical point. Finally, the distance between X and the C–X bond critical point in the TS is given (r_{C-X}).

Several observations are apparent from the data in Table I. In particular, in a series of reaction systems with the same leaving group but different entering nucleophiles, the charges on the leaving groups in the TS are not equal but correlate with ΔE and ΔH in a similar way as the bond length. That is, the charges on the leaving groups in the TS are related to the position of the TS along the reaction coordinate. The later the TS, the greater the stretching of the C–X bond and the greater the transfer of charge to the leaving group.

Comparison of atomic charges obtained by integration over atomic basins[10–12] shows that the MP2′ and MP2 values are always smaller than the RHF values. In other words, RHF overestimates electron densities around the more electronegative species. This is consistent with the tendency of the Hartree–Fock method to overestimate the importance of ionic structures.[24,25] Nevertheless, the inclusion of correlation effects at the MP2′ and MP2 levels does not alter the trends exhibited by RHF results, i.e., the charge on the leaving group is related to the position of the TS along the reaction coordinate. According to the principle of microscopic reversibility, the TS of the forward reaction is also the TS of the reverse reaction.[3] In the reverse reaction, the leaving group would be the entering nucleophile, and, therefore, the charge on the entering nucleophile is also related to the position of the TS along the reaction coordinate. Generally speaking, for asymmetric reactions, the charges on N and X are not equal in the TS.

Shaik and Pross assume that in the TS, N and X should have equal charges and that the charges are not related to the position of the TS. That is, they assume in eq 1 that ψ_1 and ψ_2 make equal contributions to the TS wave function. We do not agree with their assumption for two reasons. First, from the data in Table I it can be seen that the charges on N and X are not equal. For example, in the $(H\cdots CH_3\cdots Cl)^-$ transition structure the RHF integrated charges associated with H and Cl are −0.80 and −0.64 e, respectively, while the corresponding MP2 values are −0.72 and −0.51 e, respectively. There is no indication that extending the calculations to higher order would lead to equal charges on N and

(19) Hariharan, P. C.; Pople, J. A. *Theor. Chim. Acta* **1973**, *28*, 213.
(20) Hehre, W. J.; Radom, L.; Schleyer, P. v. R.; Pople, J. A. *Ab Initio Molecular Orbital Theory*; Wiley: New York, 1986.
(21) See, for example: Duke, A. J.; Bader, R. F. W. *Chem. Phys. Lett.* **1971**, *10*, 631. Chandrasekhar, J.; Andrade, J. G.; Schleyer, P. v. R. *J. Am. Chem. Soc.* **1981**, *103*, 5609. Bayly, C. I.; Grein, F. *Can. J. Chem.* **1988**, *66*, 149 and references therein.
(22) Biegler-König, F. W.; Bader, R. F. W.; Tang, T. *J. Comput. Chem.* **1982**, *3*, 317.
(23) Boyd, R. J.; Wang, L. C. *J. Comput. Chem.*, **1989**, in press.
(24) See, for example: McWeeny, R.; Sutcliffe, B. T. *Methods of Molecular Quantum Mechanics*; Academic Press: New York, 1969; p 61. Pilar, F. *Elementary Quantum Chemistry*; McGraw-Hill: New York, 1968; pp 491 and 517.
(25) This is clearly illustrated by a recent analysis of correlation effects in the oxygen difluoride molecule: Wang, L. C.; Boyd, R. J. *J. Chem. Phys.*, **1989**, in press.

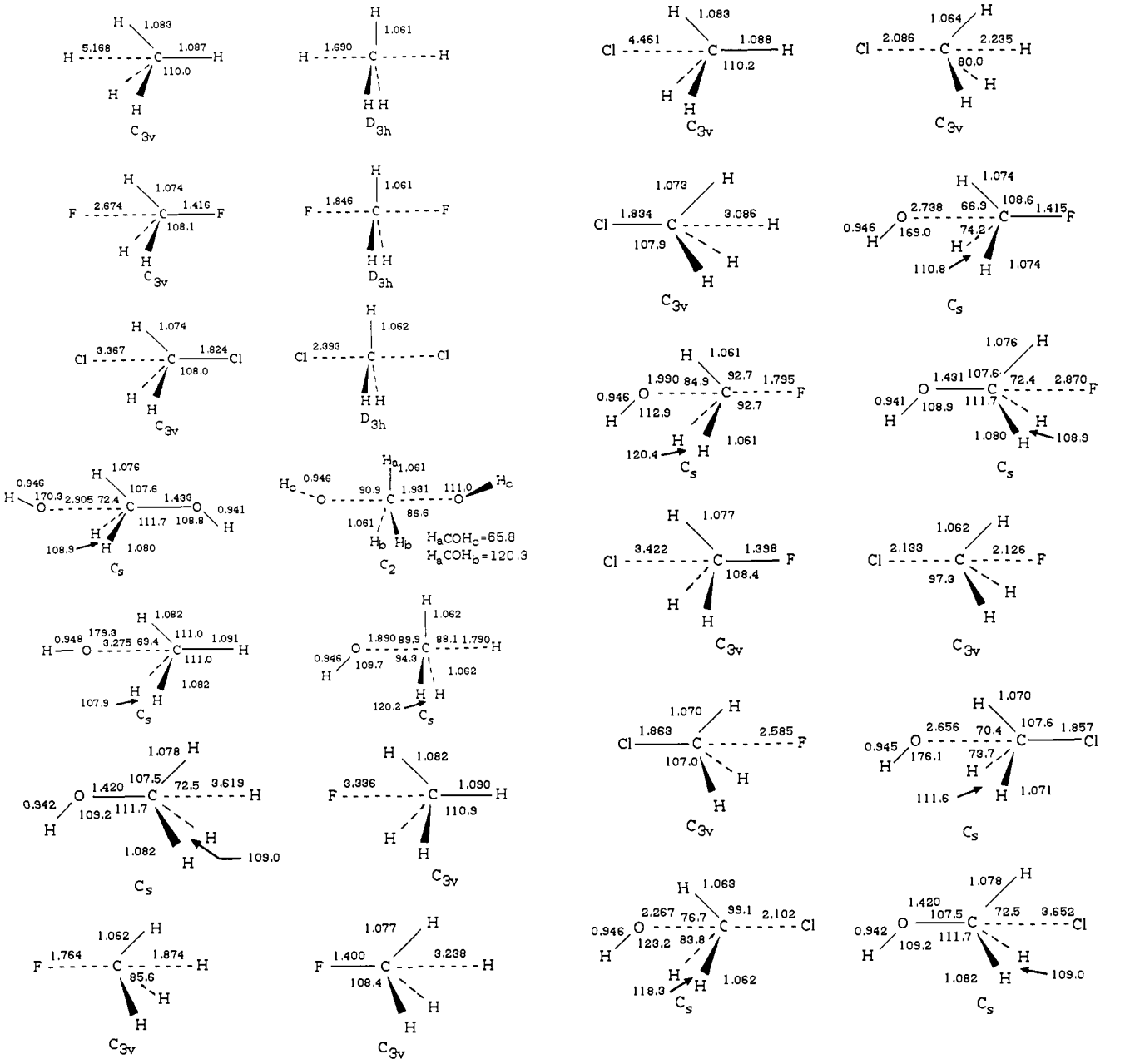

Figure 2. HF/6-31++G** optimized geometries.

X for all asymmetric transition states. We also disagree with their assumption because the wave function is a function of the nuclear coordinates, and, since the charges are determined by the wave function, it follows that the charges cannot be taken to be independent of the position of the TS.

The integrated charges obtained for the TS by application of the theory of atoms in molecules can be used to estimate upper bounds of the reactant and product configurations to the Shaik and Pross TS wave functions. The derivation is described in the Appendix, and the coefficients are listed in Table II. The results of the analysis show that c^2 is not small in the cases involving Cl and the symmetric hydride reaction. Also, for a given X, the contribution of the reactant configuration, as indicated by the value of a^2, decreases monotonically along the series H, OH, F, Cl. Similarly, for a given X, the contribution of the product configuration, as indicated by the value of b^2, increases along the series H, OH, F. For the latter series the values with Cl are anomalously low. Moreover, for a given X, the ratio of the contribution of the product configuration to that of the reactant configuration (b^2/a^2) also increases along the series H, OH, F, Cl. Bearing in mind the variation of the ΔH values (Table I), it can be seen that for a given X, the contribution of the reactant configuration decreases as the reaction becomes more endothermic. Thus, for example, with X = H, a^2 (Table II) decreases, while ΔH (Table I) increases in the series $(N\cdots CH_3\cdots H)^-$, where N = H, OH, F, Cl. This shows that the upper bounds of the contributions of Ψ_r and Ψ_p to the TS are related to the position of the TS along the reaction coordinate.

Comparison between the integrated charges in Table I and the charges based on Mulliken population analysis (MPA) indicates that the MPA values are smaller (with one exception) than the integrated values. Moreover, the MPA charges do not always show the same trends. For example, in the series $(N\cdots R\cdots H)^-$, where N = H, OH, F, Cl, as ΔH increases the integrated charge on H increases, however, the MPA charges do not increase monotonically. The plot of $-Q_X$(MPA) versus $-Q_X$(RHF), Figure 3, has a correlation coefficient of only 0.798. Deletion of the $-Q_H$ data raises the correlation coefficient to 0.976.

Proinov et al. have shown[26] that the LCAO representation of

(26) Proinov, E.; Neshev, N.; Andreev, A. *Int. J. Quantum Chem.* **1986**, *30*, 119.

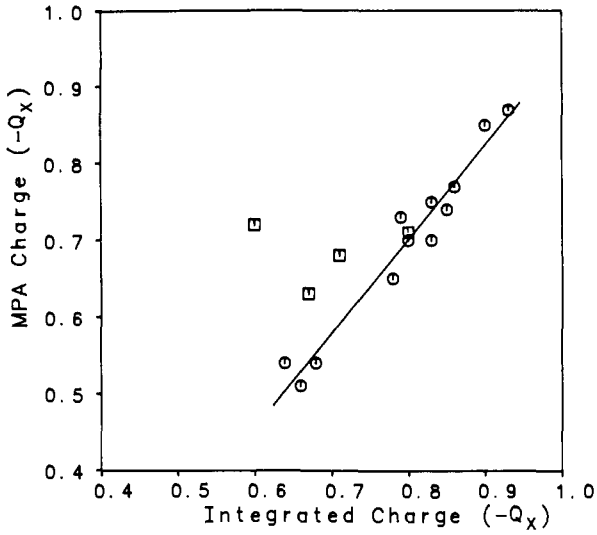

Figure 3. Correlation between the MPA charge ($-Q_X$) and the integrated charge ($-Q_X$). Charges on hydrogen atoms are denoted by □ and are deleted from the best straight line through the data points.

the atomic electron occupancy, defined via the electron occupancy of the corresponding topological atom in the molecule, is

$$N(\Omega_A) = \sum_{a\epsilon A} \tilde{q}(Aa) \int_{\Omega A} dr \varphi_{Aa}^2 \tag{2}$$

where the orbital occupancies of the topological atom are

$$\tilde{q}(Aa) = P\left(\frac{Aa}{Aa}\right) + 2 \sum_{\substack{B,b \\ B\neq A}}{}' S_{Aa,Bb} P\left(\frac{Bb}{Aa}\right) + \sum_{\substack{Bb,B'b' \\ B,B'\neq A}}{}'' S_{Aa,Bb} S_{Aa,B'b'} P\left(\frac{Bb}{B'b'}\right) \tag{3}$$

and atoms are labeled as A, B, ..., and AO's are labeled as a, b, ... The equation

$$N_A = \sum_{a\epsilon A} q(Aa) \tag{4}$$

where

$$q(Aa) = P\left(\frac{Aa}{Aa}\right) + \sum_{\substack{B,b \\ B\neq A}}{}' S_{Aa,Bb} P\left(\frac{Bb}{Aa}\right) \tag{5}$$

contains the expression for Mulliken's gross atomic populations as a special case. By comparison of eq 2 and 4, it follows that the Mulliken gross atomic population emerges as an approximation to the electron occupancy of the topological atom.[26] The topological orbital occupancies $\tilde{q}(Aa)$ are quadratic functions of the overlap integrals, whereas Mulliken's orbital occupancies are linear functions of the overlap integrals. As noted by Proinov et al.,[26] the linear two-center contribution to $\tilde{q}(Aa)$ is twice as large as the corresponding contribution to $q(Aa)$. In contrast to the equal, but arbitrary, sharing of the two-center overlap term in MPA, an appropriate sharing of the LCAO charge density is achieved by means of the topological weight factors appearing in eq 2

$$\int_{\Omega A} \varphi_{Aa}^2(r) dr = Q_{Aa} < 1 \tag{6}$$

The weight factor Q_{Aa} is directly related to the topological definition of an atom. For two atoms at infinite separation, the interatomic surface is at infinity. Hence, the integration is carried out to infinity. Thus, $Q_{Aa} = 1$, and there is no sharing of electrons between the two atoms. In the case of two directly bonded atoms, the interatomic surface passes through the bond critical point, and it is apparent that the size of an atom is related to the position of the bond critical point. Furthermore, studies[27,28] have shown

Table II. Contributions of Configurations to the TS[a]

$(N\cdots R\cdots X)^-$	a^2	b^2	c^2	d^2	b^2/a^2
$(H\cdots R\cdots H)^-$	0.40	0.40	0.20	0.00	1.00
$(HO\cdots R\cdots H)^-$	0.33	0.63	0.04	0.00	1.94
$(F\cdots R\cdots H)^-$	0.29	0.65	0.06	0.00	2.23
$(Cl\cdots R\cdots H)^-$	0.20	0.54	0.26	0.00	2.66
$(H\cdots R\cdots F)^-$	0.65	0.29	0.06	0.00	0.45
$(HO\cdots R\cdots F)^-$	0.53	0.45	0.00	0.02	0.84
$(F\cdots R\cdots F)^-$	0.49	0.49	0.00	0.01	1.00
$(Cl\cdots R\cdots F)^-$	0.29	0.47	0.24	0.00	1.65
$(H\cdots R\cdots Cl)^-$	0.54	0.20	0.26	0.00	0.38
$(HO\cdots R\cdots Cl)^-$	0.50	0.29	0.21	0.00	0.59
$(F\cdots R\cdots Cl)^-$	0.47	0.29	0.24	0.00	0.61
$(Cl\cdots R\cdots Cl)^-$	0.30	0.30	0.39	0.00	1.00
$(H\cdots R\cdots OH)^-$	0.63	0.33	0.04	0.00	0.52
$(HO\cdots R\cdots OH)^-$	0.49	0.49	0.00	0.03	1.00
$(F\cdots R\cdots OH)^-$	0.45	0.53	0.00	0.02	1.19
$(Cl\cdots R\cdots OH)^-$	0.29	0.50	0.21	0.00	1.70

[a] Results obtained at RHF level.

that the distance between an atom and its bond critical point is related to the electronegativity of the atom. The more electronegative the atom, the greater the critical radius, the more contracted the AO's, and the larger the weight factor. The result is that the two-center MO-LCAO electron density is not equally shared by the two atoms, but rather the more electronegative one has the larger share. In the Mulliken population analysis, the weight factor does not exist, and the two-center MO-LCAO electron density is assumed to be equally shared between the two atoms. As a result, the electropositive atom is assigned more electrons that it should be, whereas the more electronegative atom has less than it should have. Therefore, the MPA method usually yields smaller net charges than the integrated charges obtained from the theory[10-12] of atoms in molecules. Since the Hartree–Fock method overestimates ionic character and MPA underestimates ionic character, there is a fortuitous cancellation of errors. Hence, the charges obtained by MPA at the Hartree–Fock level are close to the integrated charges at the MP2 level (see Table I).

The data in Table I demonstrate that the electron density at the bond critical point in the TS is related to the bond length and to the position of the TS along the reaction coordinate. In a series of reaction systems with the same leaving group, as ΔH increases the TS comes later, the C–X bond length in the TS becomes longer, and the electron density at the C–X bond critical point decreases. The MP2′ and MP2 methods give similar results. However, the value of the electron density at the bond critical point is usually larger than that obtained by RHF, and the distance between the bond critical point and X is usually shorter than that obtained by RHF. As mentioned above, this phenomenon is consistent with the tendency of the Hartree–Fock method to overestimate the importance of ionic structures.[24,25]

Conclusion

Contrary to the assumption of Shaik and Pross,[8,9] self-consistent field and post-Hartree–Fock calculations indicate that for asymmetric S_N2 reactions, the entering nucleophile and the leaving group do not have equal charges in the TS. Furthermore, the charges on the entering nucleophile and the leaving group are related to the position of the TS along the reaction coordinate. The earlier the TS, the lower the amount of electron transfer.

Charges based on Mulliken population analysis are shown to be generally smaller than integrated charges obtained by application of the theory of atoms in molecules. Qualitative differences between the two sets of charges have been noted and the source of the differences explained. The integrated charges have been used to estimate upper bounds of the contributions of the reactant and product configurations to the Shaik and Pross TS wave function. It has also been shown that the electron density at the bond critical point in the TS is related to the bond length and to the position of the TS along the reaction coordinate.

(27) Boyd, R. J.; Edgecombe, K. E. *J. Am. Chem. Soc.* **1988**, *110*, 4182.

(28) Shi, Z.; Boyd, R. J., unpublished results.

Acknowledgment. A Killam Postgraduate Scholarship (to Z.S.) from Dalhousie University and the financial assistance of the Natural Sciences and Engineering Research Council of Canada in the form of an Operating Grant (to R.J.B.) are gratefully acknowledged.

Appendix

In terms of the VB configurations[8]

$$\underset{\mathbf{1}}{N{:}^{-}R{\cdot\cdot}X}, \quad \underset{\mathbf{2}}{N{\cdot\cdot}RX{:}^{-}}, \quad \underset{\mathbf{3}}{N{:}^{-}R^{+}{:}X^{-}}, \quad \underset{\mathbf{4}}{N{\cdot}R{:}^{-}{\cdot}X},$$

$$\underset{\mathbf{5}}{N{:}^{-}R{:}^{-}X^{+}}, \quad \underset{\mathbf{6}}{N^{+}R{:}^{-}X{:}^{-}}$$

the TS wave function can be written as a linear contribution as follows:

$$\Psi_{TS} = c_1\psi_1 + c_2\psi_2 + c_3\psi_3 + c_4\psi_4 + c_5\psi_5 + c_6\psi_6$$

The reactant wave function can be written[29] as a linear combination of VB configurations which contain the nucleophile N^-

$$\Psi_r = a_1\psi_1 + a_2\psi_3 + a_3\psi_5$$

and the product wave function can be written as an equivalent linear combination of VB configurations involving the leaving group X^-

$$\Psi_p = b_1\psi_2 + b_2\psi_3 + b_3\psi_6$$

The contributions of ψ_5 and ψ_6 to Ψ_{TS} are small[8] and are relatively unimportant since they involve a two-electron transfer to form high-energy configurations. Hence

$$\Psi_{TS} \approx a\Psi_r + b\Psi_p + c\psi_3 + d\psi_4 + e\psi_1 + f\psi_2$$

Although, it is not possible to determine the values of the six coefficients (a, b, c, d, e, f) from the integrated charges, it is possible to estimate the upper bounds of a and b by the following approximations. Assuming $e = f = 0$, yields

$$\Psi_{TS} = a\Psi_r + b\Psi_p + c\psi_3 + d\psi_4$$

and applying the argument of Shaik[30] yields

$$Q_X = a^2Q_{X(\Psi_r)} + b^2Q_{X(\Psi_p)} + c^2Q_{X(\psi_3)} + d^2Q_{X(\psi_4)}$$

$$Q_N = a^2Q_{N(\Psi_r)} + b^2Q_{N(\Psi_p)} + c^2Q_{N(\psi_3)} + d^2Q_{N(\psi_4)}$$

$$Q_R = a^2Q_{R(\Psi_r)} + b^2Q_{R(\Psi_p)} + c^2Q_{R(\psi_3)} + d^2Q_{R(\psi_4)}$$

$$a^2 + b^2 + c^2 + d^2 = 1$$

where $Q_{X(\Psi_x)}$ is the charge on X obtained from wave function Ψ_x. Clearly, from the net charge on the reaction system

$$Q_X + Q_N + Q_R = -1$$

Furthermore, from the VB configurations we have

$$Q_{X(\Psi_p)} = Q_{N(\Psi_r)} = -1$$

$$Q_{X(\psi_4)} = Q_{N(\psi_4)} = 0$$

$$Q_{X(\psi_3)} = Q_{N(\psi_3)} = -1$$

$$Q_{R(\psi_3)} = 1, \quad Q_{R(\psi_4)} = -1$$

$$Q_{X(\Psi_r)} = -Q_{R(\Psi_r)}$$

$$Q_{N(\Psi_p)} = -Q_{R(\Psi_p)}$$

This leads to the following three equations

$$Q_X = a^2Q_{X(\Psi_r)} - b^2 - c^2$$

$$Q_N = b^2Q_{N(\Psi_p)} - a^2 - c^2$$

$$Q_R = a^2Q_{R(\Psi_r)} + b^2Q_{R(\Psi_p)} + c^2 - d^2$$

We can obtain Q_X, Q_N, Q_R, $Q_{X(\Psi_r)}$, and $Q_{N(\Psi_p)}$ by integrating the electron density over the corresponding basin with the corresponding wave function, and finally by setting c^2 or $d^2 = 0$, we can evaluate a^2, b^2 and d^2 or c^2. In each case the choice between $c^2 = 0$ or $d^2 = 0$ is made on the basis that only one of these two possibilities yields plausible values. For example, if c^2 is set equal to zero for N = X = H, then $a^2 = b^2 = 0.60$. Clearly, $a^2 + b^2 > 1$ is unreasonable, and therefore we chose the solution given in Table II ($a^2 = b^2 = 0.40$ and $c^2 = 0.20$).

Registry No. H, 12184-88-2; CH_4, 74-82-8; HO, 14280-30-9; F, 16984-48-8; Cl, 16887-00-6; CH_3F, 593-53-3; CH_3Cl, 74-87-3; CH_4O, 67-56-1.

(29) Harcourt, R. D. THEOCHEM **1988**, *165*, 329.

(30) Reference 8, page 285.

Degenerate and Pseudodegenerate 1,3-Nitrogen Shifts in Sulfur–Nitrogen Chemistry: ^{15}N NMR Analysis of Skeletal Scrambling in $PhCN_5S_3$

Ketut T. Bestari, René T. Boeré, and Richard T. Oakley*

Contribution from the Guelph Waterloo Centre for Graduate Work in Chemistry, Department of Chemistry and Biochemistry, University of Guelph, Guelph, Ontario, N1G 2W1, Canada.
Received March 22, 1988

Abstract: Skeletal scrambling in the 1,3-NSN-bridged 5-phenyl-1,3,2,4,6-dithiatriazine ($PhCN_5S_3$) has been studied by NMR analysis of the exchange of ^{15}N-labeled nitrogen between different sites. A mechanism involving two simultaneous 1,3-nitrogen shift pathways, via carbon and sulfur, is proposed, and is supported by correlation of the observed depletion/enrichment rates with those predicted by a model based on two sets of coupled first-order site exchanges. Eyring analysis of the temperature dependence of the two first-order rate constants k_c and k_s affords activation parameters $\Delta H^{\ddagger} = 19$ (±1) kcal mol^{-1} and $\Delta S^{\ddagger} = 1$ (±5) cal mol^{-1} K^{-1} (for the carbon pathway) and $\Delta H^{\ddagger} = 22$ (±1) kcal mol^{-1} and $\Delta S^{\ddagger} = 6$ (±5) cal mol^{-1} K^{-1} (for the sulfur pathway). The barriers to both skeletal scrambling in and thermal decomposition of $PhCN_5S_3$ and related heterocycles are discussed in terms of their electronic structures.

Our understanding of the structures of molecules containing conjugated –S=N– units is based on extensive crystallographic evidence; the use of spectroscopic methods for structural analysis has been limited by the absence of convenient NMR probes. In the last decade, however, advances in both synthetic and instrumentational techniques have allowed the development of both ^{14}N

0002-7863/89/1511-1579$01.50/0